COMPARATIVE STUDY OF TWO DIFFERENT PS-INSAR APPROACHES: DEPSI VS. STAMPS.

Joaquim J. SOUSA[1,2], Andrew J. HOOPER[3] , Ramon F. HANSSEN[3] and Luisa C. BASTOS[1]

[(1)]Observatório Astronómico da Universidade do Porto, Portugal, jjsousa@utad.pt, lcbastos@fc.up.pt
[(2)]Escola de Ciências e Tecnologia, Universidade de Tras-os-Montes e Alto Douro, Vila Real, Portugal
[(3)]Institute of Earth Observation and Space Systems, Delft University of Technology, Delft The Netherlands, a.j.hooper@tudelft.nl, R.F.Hanssen@tudelft.nl

ABSTRACT

This comparative study was motivated by the results obtained from the application of two independent PS-InSAR methodologies: DePSI (Delft PS-InSAR processing package) and StaMPS (Stanford Method for Persistent Scatterers) to the Granada Basin (Southern Spain). Despite the similarity between the results obtained by both approaches, significant differences in PS density and distribution were detected.

Several experiments are performed to assess the sensitivity of both PS-InSAR approaches to different parameter settings and circumstances. The most significant differences in the processing chain of both procedures are investigated and some interesting conclusions are derived.

Finally, an adaptive PS-InSAR methodology integrating the benefits of both approaches studied is proposed from the theoretical point of view.

1. INTRODUCTION

The main purpose of this work is to derive conclusions related to both PS-InSAR methodologies, DePSI Delft PS-InSAR processing package) and StaMPS (Stanford Method for Persistent Scatterers), were applied to the Granada Basin region, located in the central sector of the Betic Cordillera (southern Spain). Detailed description of the PS-InSAR methodologies used can be found in [1] [2] [3]. Two time-series of 29 ERS-1/2 and 22 ENVISAT ASAR acquisitions covering the period from 1992 to 2006, were analysed. Rough topography of the study area associated to its moderate sismotectonic and to the geodynamic setting of this region with faults and folds in an uplifting relief by the oblique Eurasian-African plate convergence, poses a challenge for the application of interferometric techniques. Application of the PS-InSAR methodologies provided similar results; however some differences are obtained, mainly concerning PS density and location (see Fig. 1).

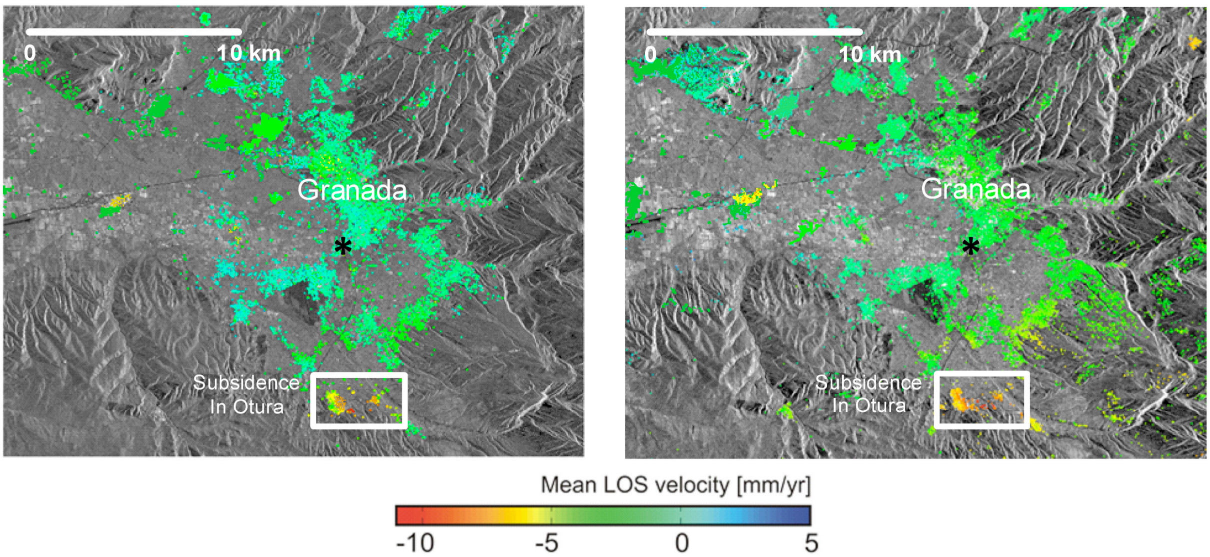

Figure 1. ERS-1/2 stack PS-InSAR results using: (left) DePSI; (right) StaMPS. A SAR mean amplitude image is used as background. The reference point is indicated by the black asterisk. The areas marked with a small white box represent the highest deformation rates (Otura village).

These observations motivated a comparative study in order to find the causes of these differences. The same area was used in each processing though the size of the area should not affect the PS density, and the same setup parameters were used (when ever possible) in the data processing.

The main difference between DePSI and StaMPS lies in the effect of the temporal smoothness assumptions (DePSI) versus spatial smoothness assumptions (StaMPS) for PS selection. In Fig. 3, some time series plots, corresponding to the PS located inside the subsidence area are shown (position of the PS point given in Fig. 2). DePSI PS time series are quite linear as expected due to the linear assumption used. PS time series of the points only selected by StaMPS (PS-C and PS-D), despite the linear behaviour shown, present a high level of noise. This may be the explanation for the fact that DePSI missed these PS.

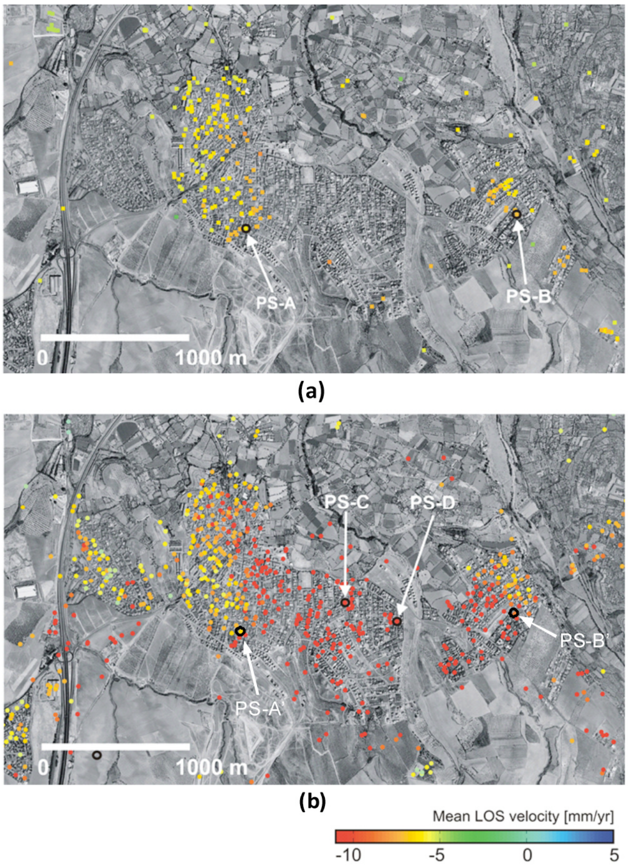

*Figure 2. PS distribution over Otura village returned by: **(a)** DePSI and **(b)** StaMPS; Some PS are selected in each image inside the subsidence bowl and their time series are represented in Figure 5.2. A 0.5 m resolution ortophoto is used as background.*

The estimated displacement rates and the quality of the compared PS (A-A´and B-B´) are listed in Tab. 1, both for DePSI and StaMPS.

The distribution of coherence values could provide some clues to explain the different results provided by both PS-InSAR methods. The coherence can be interpreted as the average closeness of the PS phase to a given model. In StaMPS, the model is the phase interpolated from surrounding pixels. In DePSI, the model is the best-fit DEM error and steady-state velocity, plus atmosphere and orbit errors interpolated from a network of PS. Fig. 4 shows a comparison of coherence magnitude for all pixels selected as PS by both methods around the Otura village. For this subset of pixels, common to both methods, the observed phase is generally closer to the model in StaMPS than in DePSI (see Fig. 4).

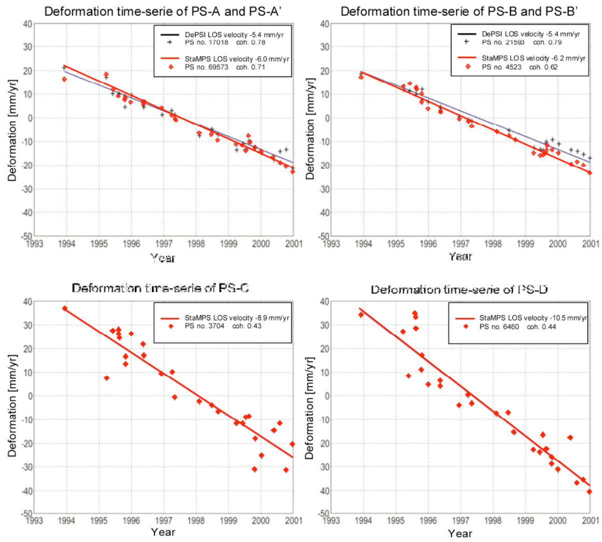

*Figure 3. Displacement time series with respect to the reference point of the PS located inside the subsidence bowl represented in Fig. 2. **(top)** Overlap of nearby points returned by DePSI (PS-A and PS-B) and returned by StaMPS (PS-A' and PS-B'). **(bottom)** Time series of PS-C and PS-D only returned by StaMPS. The positions of the PS points are given in Fig. 2.*

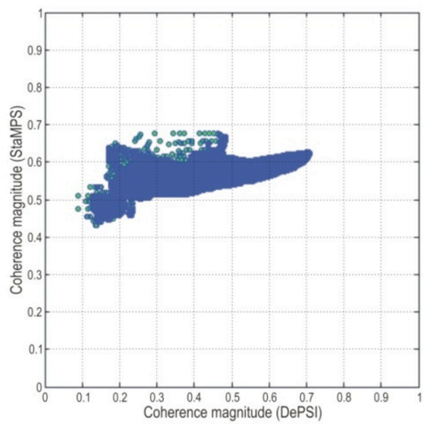

Figure 4. Comparison of coherence magnitude of common PS in Otura, selected by both methodologies.

2. COMPARATIVE STUDY

In order to understand why DePSI and StaMPS provide different results when applied to the same dataset, all the significant differences between both implementation were investigated.

2.1. Coregistration Influence

Both DePSI and StaMPS use the DORIS [4] cross correlation routines to coregister images. The difference is that DePSI does the coregistration using the traditional master-slave approach, whereas StaMPS coregisters images with small baselines and then inverts for master-slave offsets. The reason for doing this is that master-slave combinations with long baselines in rural areas often cannot be coregistered directly. The new version of DORIS (v4.01) can coregister using the DEM, which makes master-slave coregistration possible even for long baselines.

In order to evaluate the influence of this step in both approaches, the coherence between the master and the resampled slave has been computed for different registration procedures. In other words, the coherence theory is employed for SAR interferograms [5] [6] to predict the effect of interpolation on the interferogram phase quality. The average of the whole coherence crop is used as criteria to evaluate the coregistration results of DePSI and StaMPS coregistration algorithms. The resampling model was obtained based on offset vectors returned by fine coregistration that were computed at exactly the same location.

The test area was divided into different crops, covering distinct terrain occupations and each crop was processed separately. Fig. 5 shows some crops used in the tests.

As it was expected, the crops processed and presented in Fig. 5 have significant differences on the coherence values depending on the type of the soil they cover.

The coherence along the mountain slopes is generally poor, mainly due to regions affected by layover and shadow. Urban areas are in the opposite side due to the abundance of man-made constructions which behave like stable scatterers.

The mean coherence values for some of the InSAR interferograms tested are included in Tab. 1 both using DePSI and StaMPS coregistration algorithms.

2.2. Oversampling Influence

According to several authors (e.g., [2] [7]) both master and slave images should be oversampled before cross correlation to avoid aliasing due to the doubled bandwidth of the cross-correlation product compared to master and slave images. The purpose of this step is to avoid the uncorrelated contributions that would arise in the spectral cross-correlation implied by the interferogram generation, e.g. Hermitian multiplication of the two focused images [8]. The interferogram spectrum is, then, the cross-correlation of the spectra of the two images. An oversampling factor of 2 (both in azimuth and range directions) avoids aliasing in the complex multiplication of the ERS/Envisat SAR images [2]. Since the equivalent of a multiplication in the space

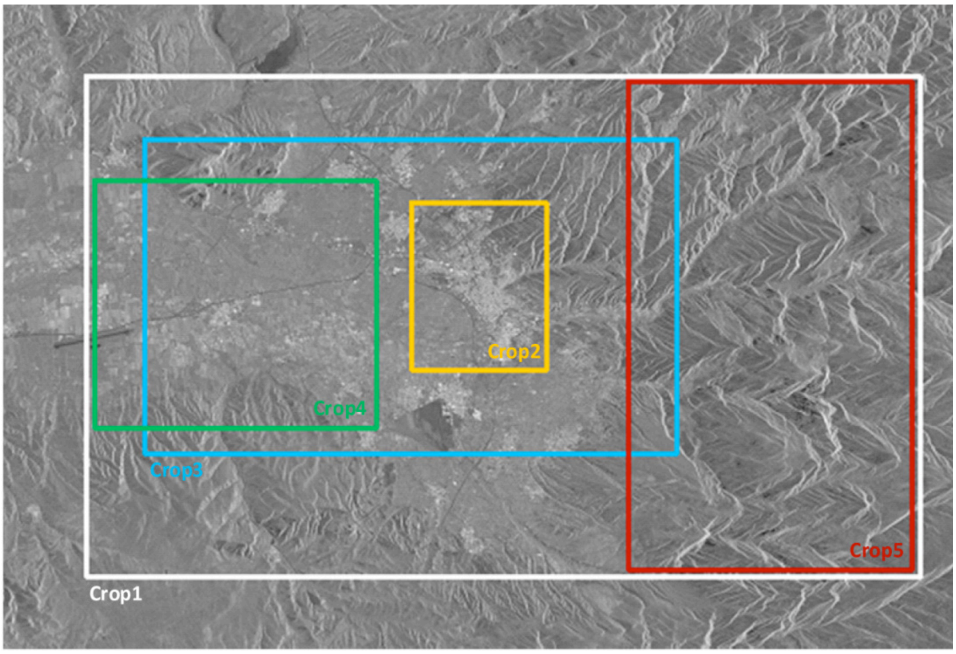

Figure 5. Different crops used to test DePSI and StaMPS coregistration procedure. Each crop covers a different area. (Crop1) Crop covering the major part of the Granada City neighbourhood (36×22 km^2); (Crop2) Crop covering (mainly) urban area (~6,4×6,8 km^2); (Crop3) Crop covering mixed areas (urban and rural – ~23×14 km^2); (Crop4) Crop covering (almost) rural areas (~13×9 km^2) and (Crop5) Crop covering mountain area (~11,3×21,3 km^2).

domain is a convolution in the frequency domain, the spectrum length will be doubled after complex multiplication of the two SAR scenes.

DePSI processing chain contemplates oversampling in its standard design. StaMPS, however, does not include this step. In order to evaluate the oversampling effect, the results supplied by StaMPS processing with and without oversampling implementation were compared.

Fig. 6 presents a set of results for the same area (Granada area) that allow checking the influence of oversampling in the final results. It is clear that the amount of PS is considerably higher when 2 factor oversampling is applied in both azimuth and range directions. In total, 7256 PS were detected without oversampling implementation against 44.189 PS when that step was considered. So, considering the implementation of oversampling will result in 6 times more PS which can be very significant when the study area is unfavourable for PS-InSAR processing as in this case. For instance, the subsidence bowl detected over Otura village is much more evident in Fig. 6b than it is in Fig. 6a.

Table 1. Mean coherence values obtained for some interferogram coregistered using the DePSI and the StaMPS coregistration implementations. The dashed rectangle highlights the interferograms with lower coherence.

Orbit	Acquisition date	$B_\perp$ (m)	ΔT (days)	Mean coherence values Crop1	Crop2	Crop3	Crop4	Crop5	PS-InSAR Method
24683	09-JAN-2000	-37	910	0.4655	0.5056	0.4735	0.4625	0.4612	DePSI
				0.4656	0.5056	0.4734	0.4625	0.4611	StaMPS
14663	08-FEV-1998	-140	210	0.4647	0.4951	0.4709	0.4618	0.4591	DePSI
				0.4647	0.4951	0.4710	0.4617	0.4591	StaMPS
05645	19-MAY-1996	198	-419	0.4571	0.4924	0.4658	0.4555	0.4508	DePSI
				0.4571	0.4925	0.4658	0.4554	0.4508	StaMPS
01637	13-AUG-1995	207	-700	0.4598	0.4980	0.4705	0.4564	0.4533	DePSI
				0.4598	0.4980	0.4706	0.4564	0.4533	StaMPS
10655	04-MAY-1997	-225	-70	0.4776	0.5057	0.4840	0.4792	0.4628	DePSI
				0.4777	0.5057	0.4841	0.4792	0.4629	StaMPS
03641	31-DEC-1995	312	-559	0.4371	0.4588	0.4424	0.4377	0.4311	DePSI
				0.4372	0.4589	0.4425	0.4378	0.4312	StaMPS
10154	30-MAR-1997	409	-105	0.4349	0.4600	0.4401	0.4348	0.4279	DePSI
				0.4352	0.4601	0.4403	0.4349	0.4280	StaMPS
28691	15-OCT-2000	582	1190	0.3679	0.3827	0.3696	0.3685	0.3654	DePSI
				0.3684	0.3828	0.3697	0.3687	0.3656	StaMPS
16667	28-JUN-1998	-702	349	0.3688	0.3841	0.3690	0.3599	0.3767	DePSI
				0.3695	0.3842	0.3692	0.3603	0.3765	StaMPS
12449	02-DEC-1993	919	-1319	0.2909	0.2806	0.2828	0.2790	0.3103	DePSI
				0.2916	0.3005	0.2921	0.2918	0.3005	StaMPS
02639	22-OCT-1995	1029	-629	0.2954	0.2944	0.2873	0.2724	0.3210	DePSI
				0.2955	0.2992	0.2967	0.2905	0.3118	StaMPS

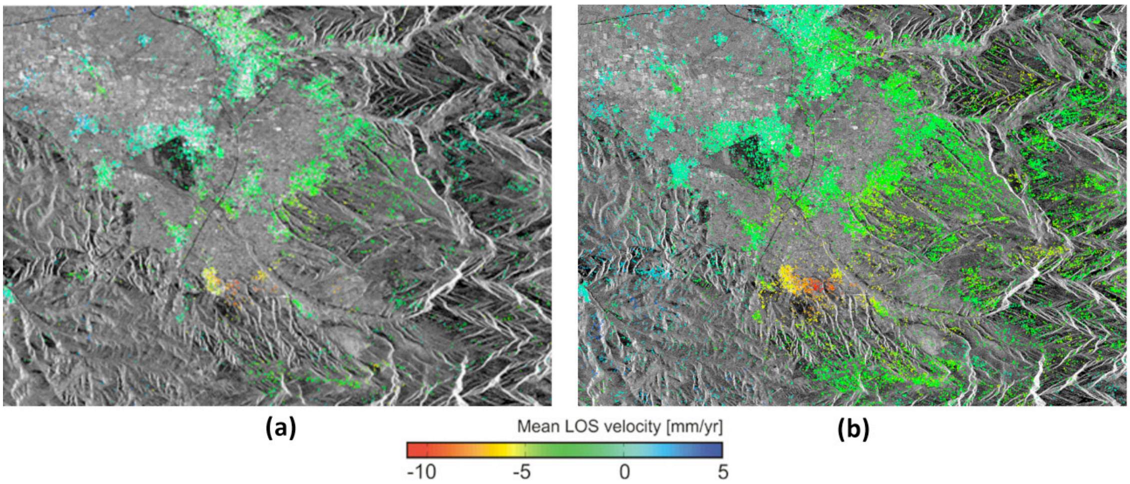

Figure 6. StaMPS processing for the Otura area. ***(a)*** *Without oversampling implementation;* ***(b)*** *With oversampling implementation.*

2.3. PS Density

The average PS density in the area of interest depends on the PS-InSAR methodology used. With DePSI the total area is covered by ~55 PS/km^2. This number drops to ~18 PS/km^2 when the standard StaMPS configuration is used. However, if oversampling is implemented in the StaMPS processing this number increases to more than 100 PS/Km^2. Evidently, these PS are not evenly distributed. The PS density is varying from up to 0-10 PS/km^2 in the rural/mountain areas to over 100 PS/km^2 in the urbanized areas. From Fig.1 it is clear that the PS distribution obtained by DePSI follows the urbanized areas. The PS targets in rural areas coincide with buildings and man-made structures. This implies that when these man-made features are absent, the PS density drops to 0 PS/km^2. For the Granada city area this is the case in more than 50% of the total area processed by DePSI. The picture is drastically different in the case of StaMPS. In general, the PS density in urbanized areas is lower than it is in DePSI (Standard processing); however, the density is significantly increased in the rural and mountain areas which constitute the main advantage of StaMPS If oversampling is implemented in the StaMPS processing chain the PS density increases so that the density in the urbanized areas is similar to the results provided by DePSI but in all the remaining covers the density is significantly higher

2.4. Influence of PS Selection Methodologies

StaMPS uses amplitude dispersion (D_A) to select PS Candidates (PSCs). Without knowing the deformation model, StaMPS filters the PSC phase in small patches in spatial and temporal dimensions separately to divide the correlated interferogram phase into incidence angle error, APS difference, deformation trends and noisy parts. The thresholds for selecting a pixel as PS are determined by calculating the PS probability of every PSC, which considers both the temporal coherence and the amplitude dispersion. After that, the deformation series are unwrapped by a three-dimensional unwrapping algorithm.

DePSI also uses amplitude dispersion to select PS candidates although in a more strict way. Only the points with stable temporal phase behaviour in time will be considered as PSC. The main objective in the selection of these (1st order) PS candidates is to establish a reference network of coherent points, which are preferably distributed homogeneously over the area of interest in order to interpolate the estimated atmospheric signal. After the formation of a network and calculation of relative phase observation per arc, the phases are unwrapped per arc in time together with the estimation of the parameters of interest. The basic task is to estimate the parameter of interest (e.g., relative deformation rate, residual height difference, etc.) and integer ambiguities from wrapped phase values. An assumption for the deformation model is necessary in this step. Without any *a priori* knowledge about deformation, a linear deformation mechanism is usually assumed.

In order to test the influence of these different approaches in the PS selection, a new dataset with particular characteristics was used. A controlled corner reflector experiment (CRE) has been set up with levelling as an independent validation technique. In the period from March 2003 to June 2004, the movements of five corner reflectors in the area near Delft University of Technology have been monitored using levelling and repeat-pass InSAR (ERS-2 and Envisat). Fig. 7 shows the CR locations.

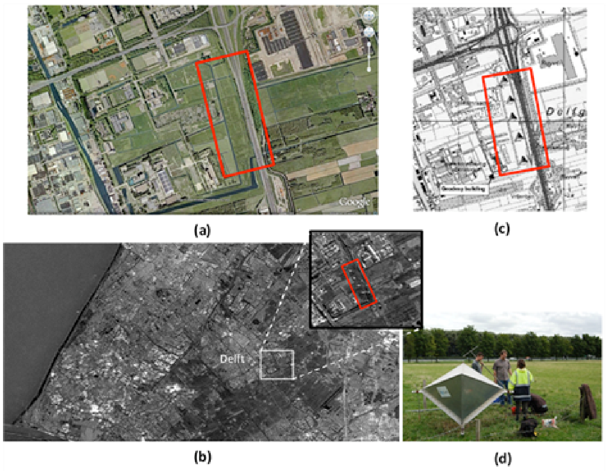

Figure 7. *The corner reflector experiment area.* ***(a)*** *Google Earth view;* ***(b)*** *A multi-image reflectivity map of Delft neighbourhood* ***(c)*** *Topographic map and details of the radar cross section of the reflectors;* ***(d)*** *Photo of one CR used in the experiment. The red rectangle delimits the CR area.*

According to the way that DePSI selects PS there is no doubt that these very bright points with a very stable phase in time will be selected as PS. But one question rises: *Will StaMPS be able to detect these points as PS?* In the first stage, when StaMPS selects PS candidates based on amplitude dispersion, it is certain that these points will be selected as well. Then, PSC will be filtered in small patches to determine the spatially-correlated phase. This is an iterative procedure that estimates the phase noise of each candidate in every interferogram. Noisy points will be discarded until convergence is achieved. According to this principle, the corner reflectors should be detectable by StaMPS. In Fig. 8, we can compare the results provided by both approaches. The general results are very similar both in density and in the relative deformations estimated. Same results and relative deformations are also derived inside the CRE area.

2.5. Computational Aspects

Both PS-InSAR approaches used in this study were run on a laptop using a 2.53 GHz processor and 4 GB of RAM memory. Due to the amount of data originated from the processing, an external hard disk was used (7200 rpm). However, computational demands are quite different depending on several processing factors. A PS-InSAR full processing generates several GB of information and is a time consuming task. Nowadays data storage is no longer considered a limiting factor.
The tests performed in this study were used to evaluate the behaviour of both PS-InSAR methodologies in terms of computational requirements. In particular, processing time and volume of data generated were analysed. All these computational aspects depend, of course, on the size and coherence of the processed area, the number of scenes available and the methodology applied. Tab.2 summarises the main computational aspects resulting from DePSI and StaMPS processing. For instance, the processing time related to Fig. 6 took 14 hours to complete the DePSI interferometric part and originated 27 GB of data.

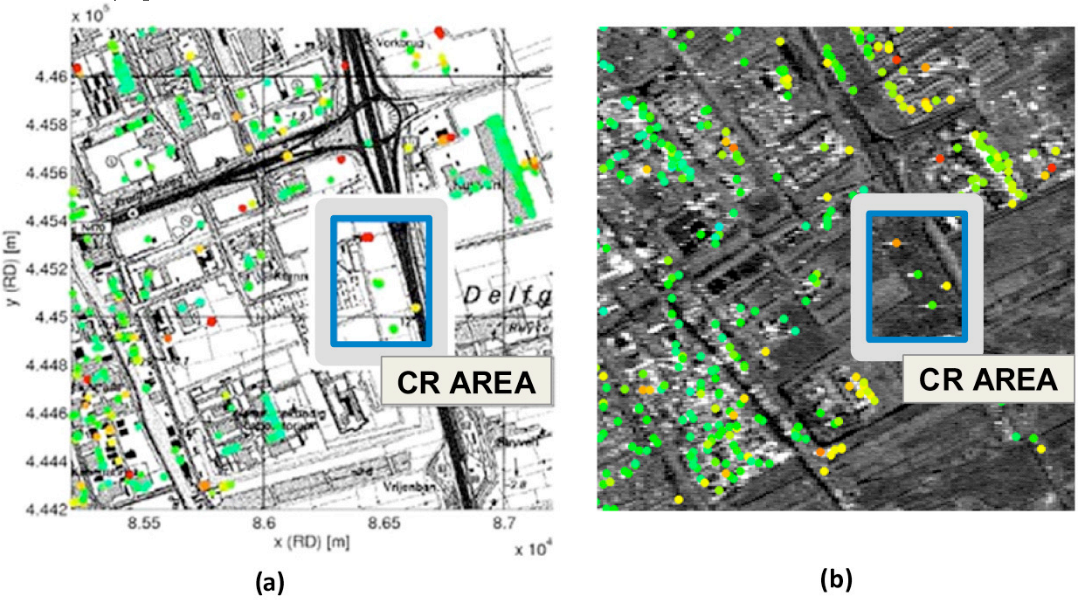

Figure 8. Linear velocities in the corner reflectors area provided by: ***(a)*** *DePSI. A topographic map is used as background (picture from [9]);* ***(b)*** *StaMPS results superimposed to a SAR amplitude image. The Linear velocities are not referred to the same reference point; although is possible to check their similarity.*

Table 2. Computational aspects evaluation for StaMPS and DePSI processing chain. The evaluation is divided in interferometric part (IFG) and PS processing part. In order to make the comparison easier, DePSI processing is used as a reference and all the other evaluated parameters are related to this value.

PS-InSAR Methodology	Time consuming						Disk space	
	IFG		PS				IFG	PS
	M-S	S-S	3D	Perio	Boot	ILS		
DePSI	1	NA	NA	1	10	NE	1	1
StaMPS (no ovs)	0.6	0.75	0.33	NA	NA	NA	0.2	0.4
StaMPS (ovs)	0.75	1	1*	NA	NA	NA	1	2.1

NA – not applicable; NE – not evaluated; 3D – Stamps 3D unwrapping;
DePSI temporal unwrapping based on: Perio – periodogram; Boot – integer bootstrapping; ILS – Integer Least Square.
(*) – To avoid memory problems the area was divided in 6 patches. This number depends on the number of PS initially selected and will significantly affect the processing time.

3. DePSI / StaMPS INTEGRATION

Depending on the type of the processing area one methodology could be more appropriate than the other. However, the ideal would be to merge the benefits of each methodology and tight them in a single methodology. The idea would be to develop an adaptive methodology that can be adjusted according to the characteristics of the processing area (coverage type, deformation regimes, etc.).

Despite the substantial improvements resulting from the new and appealing PS-InSAR methodologies, being DePSI and StaMPS two examples, there is no clear assessment of the parameterization required. The motion estimate is, indeed, a somewhat heuristic exploitation of a set of interferograms that were taken with the shortest temporal baselines possible, where the choice of the interferograms to be combined is based on a data-driven recipe that tries to get the best results, accounting for target decorrelation and atmospheric artefacts. This is also due to the fact that, up to now, no satellite has been fully dedicated to interferometry; hence, no complete sequences of interferometric images abound [10]. However, in the sequence of this study, several considerations can be summarized with the goal of integrating the advantages of both approaches into a single methodology.

After the interferometric processing, the differential interferograms should be analysed in order to select the PS candidates to start the persistent scatterers processing. Each method proved to have distinct behaviours depending on the deformation regime and land covering. Therefore, a model for target decorrelation and for providing a statistically consistent estimator to be used mainly for the assessment of the ground motion accuracy should be established. The parameters of this model can be identified using estimates of coherence. The sampled estimate may be applied to the interferogram after removing the topographic contribution by means of a digital elevation model. Typically, this estimation is done by using a window-based coherence method. However, the estimation window should be sufficiently large to minimize the bias of the estimate [11]. The result will be a series of matrices, each of them representing the temporal correlation properties in a particular place in the scene (actually, the estimation window).

StaMPS approach is essentially based on estimating the coherence matrix. The whole point of the coherence matrix is to estimate the noise associated with a pixel in each interferogram, based on it's coherence with surrounding pixels. StaMPS estimation of the noise for every pixel in every interferograms (also based on coherence with surrounding pixels) is a better estimate than the simple window-based coherence method, which can be more biased by the noise of surrounding pixels. One advantage of doing this would be to use pixels that are only sometimes coherent (e.g. where it snows). Therefore, in order to incorporate the noise estimated from spatial coherence into DePSI, the existing StaMPS algorithms should be applied.

4. CONCLUSION

A comparative study was carried out concerning both approaches used. This study was motivated by the significant differences found, mainly in PS location and density. The most significant differences in StaMPS and DePSI processing chains were investigated in order to depict the behaviour of each PS-InSAR approach according to the area and to the deformation regime. The critical procedures in the Interferometric processing were studied: SAR image coregistration and oversampling. The results from those algorithms were compared, through the experiments carried out on the Granada basin dataset. Distinct conclusions were derived. It was confirmed the benefits brought by the StaMPS coregistration method, however, these improvements did not revealed to be significant in the case where the study area presents a reasonable correlation, even if long perpendicular baselines are used.

Another significant difference in the interferometric (part) processing regards the oversampling step. StaMPS, contrary to DePSI, does not include this step on its standard design. The benefits from the inclusion of the oversampling step in StaMPS were evaluated and the results demonstrated that significant improvements, mainly in the PS density, are obtained.

Finally, the PS processing part is also distinct in each methodology therefore, they were also analysed and evaluated with the purpose of proposing a methodology that integrates the benefits of both. It was concluded that StaMPS and DePSI are complementary in different aspects like is the case of PS selection and unwrapping which can be use to improve the results. Urbanized areas, more coherent, are better analysed by DePSI due to the man-made structures while StaMPS presents a favourable behaviour in the other types of areas, less coherent. Despite these differences, some of them significant, the general deformation framework has been detected by both approaches when applied to the Granada basin dataset.

5. REFERENCES

1. Kampes, B. M. (2005). Displacement Parameter Estimation using Permanent Scatterer Interferometry, *PhD Thesis*, Delft University of Technology.

2. Ketelaar, V. B. H. (2008). Monitoring Surface Deformation Induced by Hydrocarbon Production using Satellite Radar Interferometry. *PhD. Thesis*, Delft Institute of Earth Observation and Space Systems, TUDelft.

3. Hooper, A., Segall, P. and Zebker, H. (2007). Persistent Scatterer InSAR for Crustal Deformation Analysis, with Application to Volcán Alcedo, Galápagos. *Journal of Geophysical Research*, vol. XXX, XXXX, DOI:10.1029/2006JB004763, 2007.

4. Kampes, B. and Usai, E. (1999). Doris: the Delft Object-Oriented Radar Interferometric Software. *In 2nd International Symposium on Operationalization of Remote Sensing*, Enschede, The Netherlands, 16-20 August, 1999.

5. Just, D. and Bamler, R. (1994). Phase Statistics of Interferograms with Applications to Synthetic Aperture Radar. *Applied Optics*, Vol. 33, No. 20, pp.4361-4368.

6. Cattabeni M., Monti-Guarnieri A., Rocca F. (1994). Estimation and Improvement of Coherence in SAR Interferograms. *Proceedings of IGARSS 94*, Pasadena, California.

7. Ferretti, A., Monti-Guarnieri, A., Prati, C., Rocca, F. (2007). InSAR Principles: Guidelines for SAR Interferometry Processing and Interpretation. *ESA Publications, TM-19*, February 2007.

8. Gatelli, F., Monti Guarnieri, A., Parizzi, F., Pasquali, P., Prati, C., Rocca, F. (1994). The Wavenumber Shift in SAR Interferometry. *IEEE Transactions on Geoscience and Remote Sensing*, 32 (4), pp. 855-865.

9. Marinkovic, P., Ketelaar, G., van Leijen, F. and Hanssen, R (2007). InSAR Quality Control: Analysis of Five Years of Corner Reflectors Time Series. *Fringe Workshop 2007*. Frascati, 26-30 November 2007, Italy.

10. Drezet ,P. M. L. and Quegan, S. (2006). Environmental effects on the interferometric repeat-pass coherence of forests. *IEEE Trans. Geosci. Remote Sens.*, vol. 44, no. 4, pp. 825–837, Apr. 2006.

11. Touzi, R.; Lopes, A.; Bruniquel, J. and Vachon, P. W. (1999). Coherence estimation for SAR imagery. *IEEE Trans. Geosci. Remote Sens.*, vol. 37, no. 1, pp. 135–149, Jan. 1999.